Environmental Research 231 (2023) 116068

Contents lists available at ScienceDirect

Environmental Research

journal homepage: www.elsevier.com/locate/envres

Snapshots of wintertime urban aerosol characteristics: Local sources emphasized in ultrafine particle number and lung deposited surface area

Teemu Lepistö [a,*], Luis M.F. Barreira [b], Aku Helin [b], Jarkko V. Niemi [c], Niina Kuittinen [a], Henna Lintusaari [a], Ville Silvonen [a], Lassi Markkula [a], Hanna E. Manninen [c], Hilkka Timonen [b], Pasi Jalava [d], Sanna Saarikoski [b], Topi Rönkkö [a]

[a] Aerosol Physics Laboratory, Physics Unit, Faculty of Engineering and Natural Sciences, Tampere University, Tampere, 33014, Finland
[b] Atmospheric Composition Research, Finnish Meteorological Institute, Helsinki, 00101, Finland
[c] Helsinki Region Environmental Services Authority HSY, Helsinki, 00066, Finland
[d] Inhalation Toxicology Laboratory, Department of Environmental and Biological Sciences, University of Eastern Finland, Kuopio, 70211, Finland

ARTICLE INFO

Handling Editor: Jose L Domingo

Keywords:
Ultrafine particles
Mobile laboratory
Traffic
Biomass burning
Airport
Human respiratory tract

ABSTRACT

Urban air fine particles are a major health-relating problem. However, it is not well understood how the health-relevant features of fine particles should be monitored. Limitations of $PM_{2.5}$ (mass concentration of sub 2.5 μm particles), which is commonly used in the health effect estimations, have been recognized and, e.g., World Health Organization (WHO) has released good practice statements for particle number (PN) and black carbon (BC) concentrations (2021). In this study, a characterization of urban wintertime aerosol was done in three environments: a detached housing area with residential wood combustion, traffic-influenced streets in a city centre and near an airport. The particle characteristics varied significantly between the locations, resulting different average particle sizes causing lung deposited surface area (LDSA). Near the airport, departing planes had a major contribution on PN, and most particles were smaller than 10 nm, similarly as in the city centre. The high hourly mean PN (>20 000 1/cm^3) stated in the WHO's good practices was clearly exceeded near the airport and in the city centre, even though traffic rates were reduced due to a SARS-CoV-2-related partial lockdown. In the residential area, wood combustion increased both BC and $PM_{2.5}$, but also PN of sub 10 and 23 nm particles. The high concentrations of sub 10 nm particles in all the locations show the importance of the chosen lower size limit of PN measurement, e.g., WHO states that the lower limit should be 10 nm or smaller. Furthermore, due to ultrafine particle emissions, LDSA per unit $PM_{2.5}$ was 1.4 and 2.4 times higher near the airport than in the city centre and the residential area, respectively, indicating that health effects of $PM_{2.5}$ depend on urban environment as well as conditions, and emphasizing the importance of PN monitoring in terms of health effects related to local pollution sources.

This work was supported by the European Union's Horizon 2020 research and innovation programme under grant agreement No 814978 (TUBE: Transport-derived ultrafines and the brain effects); BC Footprint project (530/31/2019) funded by Business Finland, participating companies and municipal actors; Academy of Finland Flagship funding Atmosphere and Climate Competence Centre, ACCC (grant no. 337552, 337 551); and Finnish Foundation for Technology Promotion.

The study does not involve human nor animal subjects.

1. Introduction

Urban air pollution is a major climate- and health-related problem worldwide. One of the main contributors on urban air pollution and its effects is fine particulate matter (particles with a diameter smaller than 2.5 μm). Fine particles have been estimated to cause millions of premature deaths globally, and the estimates vary e.g., between 3.3 and 10.2 million premature deaths per year (Lelieveld et al., 2015; Cohen et al., 2017; Vohra et al., 2021). Other major contributors on urban air quality are e.g., nitrogen dioxide (NO_2), sulphur dioxide, ozone, and carbon monoxide. Exposure to different air pollutants is typically the

* Corresponding author. Korkeakoulunkatu 3, 33720, Tampere, Finland, P.O.Box 692, 33014 Tampere, Finland.
E-mail address: teemu.lepisto@tuni.fi (T. Lepistö).

https://doi.org/10.1016/j.envres.2023.116068
Received 26 October 2022; Received in revised form 14 April 2023; Accepted 4 May 2023
Available online 5 May 2023
0013-9351/© 2023 The Authors. Published by Elsevier Inc. This is an open access article under the CC BY license (http://creativecommons.org/licenses/by/4.0/).

highest in cities where various sources of atmospheric pollutants are combined with high population density. Emissions e.g., from traffic and biomass combustion can worsen urban air quality (Saarikoski et al., 2021), but air quality is also depended on distant emissions sources and long-range transported (LRT) aerosol (e.g., Pirjola et al., 2017).

Over the years, urban air quality has been considered in legislation and there are regulations regarding the concentrations of different pollutants. Due to these regulations on atmospheric concentrations as well as due to emission limits for individual pollutant sources, air quality has improved e.g., in Europe (Sicard et al., 2021). However, pollutants and fine particulate matter still cause hundreds of thousands of premature deaths annually in Europe (EEA, 2021; Sicard et al., 2021).

Health effects of fine particles are often associated with $PM_{2.5}$ (e.g., Dockery et al., 1993; Burnett et al., 2014), which is the mass concentration of particles with a diameter smaller than 2.5 μm. In fact, $PM_{2.5}$, alongside with PM_{10} (diameter smaller than 10 μm), is the main metric for particulate pollution in the World Health Organization's (WHO) global air quality guidelines (WHO, 2021) and in legislation (Gemmer and Xiao, 2013). For example, WHO's $PM_{2.5}$ guideline levels for 24-h and annual mean concentrations are 15 and 5 $\mu g/m^3$, respectively. Current legislation assumes all particle mass concentrations as equally harmful, even though the association between the premature deaths and $PM_{2.5}$ depends on the country (Li et al., 2019). Also, there are major differences in chemical composition as well as in mass- and number size distributions within the $PM_{2.5}$ (e.g., Pirjola et al., 2017), emphasizing the need to understand the characteristics of the local fine particulate matter in terms of health effects. Furthermore, most urban air fine particles are ultrafine, i.e., smaller than 100 nm (e.g., Kumar et al., 2010). Due to the small size, ultrafine particles do not contribute to $PM_{2.5}$ notably as their mass is insignificant. Thus, there is a need for different metrics, alongside with $PM_{2.5}$, when estimating the health effects caused by local particle pollution.

In addition to $PM_{2.5}$, particle concentrations can be monitored e.g., with ultrafine particle number (PN) concentration and black carbon (BC) mass concentration. As most urban air particles are smaller than 100 nm, the local emissions (e.g., traffic) are usually more easily detected with PN than with $PM_{2.5}$. In a review study by Ohlwein et al. (2019), ultrafine particles were linked to short-term effects on human health such as changes in inflammatory status and cardiovascular conditions. Despite the evidence on negative health effects, there is still a large need for more quantitative evidence on the individual health impacts of PN. For example, the lower limit of the measured size range of ultrafine particles significantly affects the measured PN, and this lower measurement limit varies usually from a couple of nanometres up to 23 nm, depending on the study. Also, the EU emission standards for vehicle emission consider 23 nm as the lower limit for PN of solid particles even though most of the emitted particles are smaller (Rönkkö et al., 2017). In the new WHO, 2021 air quality guidelines, monitoring of PN has been introduced as a good practice statement, but WHO decided not yet to formulate guideline levels for PN concentration. However, WHO recommends distinguishing between low and high PN concentrations to guide the decisions on the priorities of ultrafine particle emission source control. PN concentrations higher than 10 000 $1/cm^3$ (24-h mean) and 20 000 $1/cm^3$ (1-h mean) can be considered as high PN concentration. WHO also stated that the lower limit of the measurement size range should be 10 nm or smaller.

Ambient black carbon is one of the main components of the ambient particulate matter. BC is emitted from incomplete combustion processes and, therefore, it is a good tracer for emissions e.g., from traffic and biomass combustion. In addition, BC can induce adverse health effects by itself or by carrying other harmful components on its surface into the human respiratory tract (e.g., Cassee et al., 2013). Thus, BC is an important metric when considering the health effects of local combustion emissions. Typically, the fraction of BC in urban air $PM_{2.5}$ is 5–20%, depending on the environment (Luoma et al., 2021). It has been found that the association between the negative health effects (e.g., cardiovascular diseases) and BC may be stronger than the respective association with $PM_{2.5}$ (Janssen et al., 2011). Monitoring of BC has also been added to the new WHO guidelines (WHO, 2021) as a good practice statement, similarly as PN. However, exact limits for high BC concentration are not provided, and the urgent need for new research-based information, systematic measurements, emission inventories, and source apportionment is indicated.

As all the mentioned metrics ($PM_{2.5}$, PN, BC) emphasize certain features of ambient fine particles, it is important to understand, which metrics are the most important in terms of air quality and adverse health effects. One option to estimate the potential negative health effects of fine particles is the measurement of lung deposited surface area (LDSA) of particles. LDSA estimates the surface area concentration of particles that deposit in the alveolar region of the human respiratory tract. It has been found that the surface area could be the most relevant feature when considering the health effects of ultrafine particles (Brown et al., 2001, Oberdorster et al., 2005). The alveolar region is considered crucial as the interaction between the respiration and the pulmonary circulation occurs there. It has been observed that the association between the negative health effects (Aguilera et al., 2016; Patel et al., 2018), including mortality (Hennig et al., 2018), and LDSA could be stronger than with $PM_{2.5}$ or PM_{10}. Thus, LDSA is another very potential tracer to analyse health effects caused by fine particles. Also, particle deposition in other regions of the human respiratory tract, e.g., in head airways, could cause adverse health effects. For example, there is a risk that particles could damage the human brain by entering directly through the olfactory nerve (Maher et al., 2016). Also, long-term exposure to fine particles increases e.g., the risk of Alzheimer's disease (Jung et al. 2015), indicating that fine particles have effects on the human brain.

To understand how urban air fine particles should be monitored and regulated in terms of health effects, it is necessary to know how the fine particle characteristics depend on the urban environment, and how the different particle metrics can detect the health-relevant features of the particulate pollution. In our study, we analysed short-term physical and chemical characteristics of wintertime aerosol in different urban environments in the Helsinki metropolitan area, Finland. The chosen environments were a detached housing area with residential wood combustion, traffic-influenced streets in the city centre, and an airport. The objective was to understand the features and effects of different emissions sources in terms of air quality and possible health effects. The sizes and concentrations of particles were analysed in detail by measuring PN separately for particles larger than 2.5 nm, 10 nm, and 23 nm, including size distributions in the size range of 2.5 nm–2.5 μm. Furthermore, the volatility of particles was analysed by utilizing a thermal treatment in the sample line. Previous studies of the in-detail characteristics of sub 23 and 10 nm particles have mainly considered road traffic, according to our knowledge. In addition, $PM_{2.5}$ and BC concentrations as well as the chemical composition and morphology of particles were analysed. The potential health effects of fine particles are discussed by estimating particle respiratory tract deposition, including LDSA concentrations and size distributions. According to our knowledge, the characteristics and sizes of particles causing LDSA near airports have not been analysed in previous studies. Also, the concentrations of CO_2 and NO_x were measured. We provide estimations of emission factors for ambient $PM_{2.5}$, PN, BC and NO_x, and for non-volatile $PM_{2.5}$ and PN.

2. Materials and methods

2.1. Measurement locations and campaign conditions

The measurements were conducted in a detached housing residential area, in the city centre, and next to an airport in the Helsinki metropolitan area (population ~1.2 million) on March 1st – 11th, 2021 (Fig. 1). Measurements were done by focusing on one location on each measurement day (8 a.m.–10 p.m.) by utilizing the Aerosol and Trace-

Fig. 1. Measurement locations on map. The stationary measurement locations are marked with circles (black: urban background, brown: residential area, red: street canyon, blue: airport). The driving route in the city centre is marked with a red line. Furthermore, pictures from the street canyon, Airport B, and residential area measurement sites are provided.

gas mobile laboratory (ATMo-Lab, e.g., Rönkkö et al., 2017; Lepistö et al., 2022) in both stationary and driving measurements. The measurement days, locations, and weather conditions are shown in Table 1. During the campaign, ambient temperature varied between −11.6 °C and +4.1 °C, and wind speed was mainly moderate.

The residential area measurements were conducted as stationary measurements in Ruskeasanta, Vantaa (60.3120 N, 25.0110 E). Ruskeasanta is a detached housing area where residential wood combustion is common in fireplaces and sauna-stoves. The site is approximately 700 m away from Tuusulanväylä highway (48 100 vehicles/day, Finnish Transport and Infrastructure Agency). The closest runway of Helsinki-Vantaa airport (~4.3 million passengers in 2021, Finavia) is approximately 1500 m away.

The measurements in the city centre were conducted as both stationary and driving measurements. The stationary location was on a kerbside in Mäkelänkatu street canyon next to an air quality monitoring supersite (60.1963 N, 24.9523 E) operated by Helsinki Region Environmental Services Authority (HSY). In 2019, an average traffic rate on the street (Mäkelänkatu) was 28 000 vehicles/day on weekdays, but during the campaign, SARS-CoV-2-related partial lockdown significantly reduced the traffic rates. The canyon is 42 m wide and buildings on both sides are 17 m tall, weakening the dilution process of pollutants (Karttunen et al., 2020, see also Barreira et al., 2021). The driving measurement route consisted of the main streets in the Helsinki city centre, including the street canyon (Mäkelänkatu) and e.g., traffic-light junctions, traffic-jams, street canyons and sidewalks, as well as a park section and a short stationary urban background measurement next to the sea in Hietaniemi (60.1722 N, 24.9040 E). However, the concentrations measured in the park section and the background site were not included when analysing the results of the city centre driving measurements.

Next to Helsinki-Vantaa airport, two measurement sites were utilized depending on the wind direction. The location A (60.3140 N, 24.9917 E) was south-east from the airport, approximately 500 m away from runway 2. The location B (60.3196 N, 24.9133 E) was west from the airport, approximately 200 m away from runway 3. During the measurements, the closest roads, Katriinantie (4700 vehicles/day) and Tuusulanväylä, were in upwind directions, thus not significantly affecting the measurements. The aircrafts departed mainly from the runway 3. Due to the SARS-CoV-2 outbreak, air traffic was significantly reduced during the campaign. The measurements in both locations were mainly done during times when the activity in the airport was close to the typical day-time activity before the outbreak (take-offs approximately every 5 min). Otherwise, the measurements were done in the residential area during the airport measurement days.

In addition to the measurements during March 1st – 11th, a short measurement to characterize emissions of a coffee roastery (see Timonen et al., 2013; Carbone et al., 2014; Kuula et al., 2020) near the street canyon was conducted with the same setup on March 15th. Due to the relatively short campaign period and varying conditions, the results of this study should be considered as snapshots of urban wintertime aerosol in certain locations and during certain conditions and should not be generalized as average long-term characteristics of urban aerosol in the studied sites. The presented results are selected from periods when the contribution of the local emissions was clear to understand the in-detail effects of the studied pollution sources. The amount of data in each of the studied locations is provided in Supplementary (Table S1).

2.2. Measurement setup and instruments

The measurements were conducted with the ATMo-Lab measurement van. In the ATMo-Lab, the sample was taken in the front of the car above the windshield at the height of 2.2 m, and then divided for the instruments installed in the back end of the van.

The particle number concentrations were measured with a CPC battery, i.e., parallel Condensation Particle Counters (CPC) with different cut-off diameters (2.5 nm (TSI 3756), 10 nm (Airmodus A20) and 23 nm (Airmodus A23)). A bifurcated flow diluter (dilution ratio 14) was used to reduce the measured particle concentrations with the CPCs. Particle mass concentration and number size distributions were measured with an electrical low-pressure impactor (ELPI+, Dekati Oyj, Keskinen et al., 1992; Järvinen et al., 2014). In the ELPI+, particle size distributions are measured as a function of the aerodynamic diameter in the size range from 6 nm to 10 μm. Furthermore, the ELPI + enables an accurate measurement of LDSA concentration and size distribution in the whole measurement size range (Lepistö et al., 2020), which differs from the typical sensor based LDSA measurement (e.g., Fissan et al., 2006; Fierz et al., 2014) which is reasonably accurate only for

Table 1
Campaign measurement days, measurement times and average weather conditions (temperature (T), wind direction, wind speed and relative humidity (RH)) during measurement days (8 a.m.–5 p.m.) and evenings (5 p.m.–10 p.m.). Measurements were not conducted on March 7th.

Day March 2021	Time of the day	Measurement locations	T (°C)	Wind direction	Wind Speed (m/s)	RH (%)
Mon 1st	Day (8 a.m.–5 p.m.)	Residential area	*+3.1*	*West*	*4.1*	*78*
	Evening (5 p.m.–10 p.m.)	Residential area	*+4.1*	*West*	*5.3*	*71*
Tue 2nd	Day (8 a.m.–5 p.m.)	Street canyon	*+3.7*	*North-west*	*7.2*	*66*
	Evening (5 p.m.–10 p.m.)	Street canyon	*+2.4*	*West*	*5.1*	*70*
Wed 3rd	Day (8 a.m.–5 p.m.)	Residential area & Airport A	*+3.2*	*West*	*5.6*	*70*
	Evening (5 p.m.–10 p.m.)	Residential area	*+3.5*	*West*	*6.0*	*80*
Thu 4th	Day (8 a.m.–5 p.m.)	Residential area & Airport A	*−1.6*	*North-west*	*5.6*	*61*
	Evening (5 p.m.–10 p.m.)	Residential area	*−3.3*	*North-west*	*3.8*	*81*
Fri 5th	Day (8 a.m.–5 p.m.)	Residential area & Airport A	*−4.0*	*North-west*	*5.0*	*54*
	Evening (5 p.m.–10 p.m.)	Residential area	*−5.0*	*North-west*	*3.7*	*61*
Sat 6th	Day (8 a.m.–5 p.m.)	Residential area & Airport A	*−0.4*	*North-west*	*7.1*	*86*
	Evening (5 p.m.–10 p.m.)	Residential area	*+1.3*	*West*	*6.8*	*84*
Sun 7th						
Mon 8th	Day (8 a.m.–5 p.m.)	Street canyon	*−8.8*	*North-west*	*4.6*	*57*
	Evening (5 p.m.–10 p.m.)	Street canyon	*−5.6*	*North-west*	*1.9*	*58*
Tue 9th	Day (8 a.m.–5 p.m.)	Residential area & Airport B	*−10.5*	*East*	*6.9*	*88*
	Evening (5 p.m.–10 p.m.)	Residential area	*−11.6*	*North-east*	*8.0*	*77*
Wed 10th	Day (8 a.m.–5 p.m.)	Residential area & Airport B	*−11.6*	*East*	*6.3*	*64*
	Evening (5 p.m.–10 p.m.)	Residential area	*−11.6*	*East*	*4.9*	*68*
Thu 11th	Day (8 a.m.–5 p.m.)	Street canyon	*−4.0*	*South-east*	*6.8*	*84*
	Evening (5 p.m.–10 p.m.)	–	*−2.0*	*South-east*	*8.8*	*67*

approximately 20–400 nm particles (e.g., Todea et al., 2015).

Particle chemical composition was analysed with a Soot Particle Aerosol Mass Spectrometer (SP-AMS, Aerodyne Research Inc, Billerica, US; Onasch et al. (2012)). In this study, the SP-AMS was operated with a 15 s time-resolution near the airport and during the city centre driving measurements, and with a 60 s time-resolution in stationary measurements (residential area and street canyon). When driving and in near airport measurements a mass spectra mode was used to obtain the nitrate-equivalent concentration of the measured constituents (Jimenez et al., 2003; Canagaratna et al., 2007). During the stationary measurements, a half of the measurement time the instrument operated in a Particle Time-of-Flight mode to obtain size distributions.

Ambient black carbon (BC) was measured with an AE33 Aethalometer (Magee Scientific, Drinovec et al., 2015), which determines BC mass concentration by measuring the attenuation of light at the wavelength of 880 nm. Data from other wavelengths (370–950 nm) were utilized in source apportionment analysis by calculating the absorption Ångström exponent (AAE) (Sandradewi et al., 2008). For example, AAE of traffic-influenced aerosol is typically ~1 (Kirchstetter et al., 2004; Helin et al., 2018), whereas AAE of biomass combustion influenced aerosol can be 1.1–2.2 (Helin et al. 2018, 2021). The calculation method for AAE and source apportionment analysis (Zotter et al., 2017) is shown in Supplementary (Equation S1).

Particle elemental composition and morphology was investigated by collecting particles after thermal treatment onto holey-carbon grids by utilizing a flow-through sampler. The collected particles were then analysed with a (Scanning) Transmission Electron Microscope (S/TEM, Jeol JEM-F200). The particle morphology was analysed with TEM and the elemental composition was investigated by an energy-dispersive spectrometry (EDS) included in the S/TEM. Several particle samples were collected in each studied environment during the measurements.

The non-volatile aerosol particle fraction was investigated by using a thermodenuder (Heikkilä et al., 2009; Amanatidis et al., 2018), where the sample is heated up to temperature of 265 °C causing the evaporation of the volatile particle compounds which are then collected into an active charcoal filter. Thus, only the non-volatile particle cores are left in the sample after the thermodenuder. During the measurements, the thermal treatment was switched on and off to study both ambient and non-volatile particles in turns. The thermal treatment was used in front of the CPCs, ELPI+ and particle collection (S/TEM) in the sample line.

CO_2 and NOx concentrations were measured with a LI-COR LI-7000 and a Teledyne Model T201, respectively. Regional background concentrations of $PM_{2.5}$ and BC (measured with a MAAP, Thermo Electron Corporation) were measured in HSY's rural background site in Luukki, locating approximately 18 km west from the residential area, 20 km north-west from the street canyon and 15 km west from the airport. The weather data is from Helsinki-Vantaa airport. A backward wind trajectory-analysis was done by using the National Oceanic and Atmospheric Administration's (NOAA) HYSPLIT-model (Stein et al., 2015; Rolph et al., 2017).

2.3. Data processing

The upper limit of the particle size range was chosen to be 2.5 μm to reduce uncertainties related to inertial particle losses in the sampling system of the ATMo-Lab. The reported particle number concentrations and size distributions have been corrected by estimating the particle losses due to diffusion according to the equations reported by Willeke

and Baron (2005). Particle losses in the thermodenuder were corrected according to the calibration by Heikkilä et al. (2009). The presented results were calculated by using a 1-min arithmetic mean of the measured concentrations.

With the ELPI + data, the particle effective density was assumed to be 1 g/cm^3. For example, Rissler et al. (2014) reported effective densities of 0.66–1.38 g/cm^3 for 100 nm particles in urban air. Also, the potential effects of particle hygroscopic growth in the human respiratory tract were assumed to be negligible, which is a common approximation. With traffic-originated particles, this approximation can lead to slightly overestimated lung deposition of particles smaller than 200 nm and underestimated lung deposition of particles larger than 200 nm. In the residential area, the hygroscopicity-related uncertainties can be assumed to be insignificant (Kristensson et al., 2013). The particle size distributions are presented as a function of the aerodynamic diameter based on the ELPI + measurement. However, one additional size fraction was added in the number size distributions for sub 10 nm particles based on the measured concentration difference between the CPCs with cut-off sizes of 2.5 nm and 10 nm.

A source apportionment analysis of organic aerosol (OA) was performed with the residential area data. The OA at the residential area was divided into four factors: biomass burning OA (BBOA), hydrocarbon-like OA (OA), semi-volatile oxygenated OA (SV-OOA) and low-volatility oxygenated OA (LV-OOA). Similar factors have been identified in another residential suburban area in Helsinki (Teinilä et al., 2022). The OA source apportionment was also made with the street canyon and the airport data, but they are not shown as they did not provide any additional information about the sources of ultrafine particles at those locations.

Furthermore, emission factors of ambient $PM_{2.5}$, PN, BC and NO_x, and non-volatile $PM_{2.5}$ and PN from road and air traffic were calculated by analysing their relationship with simultaneously measured CO_2 concentration. In-detail calculation method for emission factors is shown in Supplementary (Equations S2-3).

3. Results and discussion

3.1. General overview

The average measured $PM_{2.5}$ and BC during the measurement days and evenings, as well as the average regional background concentrations from the rural background site, are shown in Fig. 2. The average chemical composition of submicron particles measured with the SP-AMS is in Supplementary (Fig. S1-2). During the first eight days of the campaign when the wind was from the west, the background $PM_{2.5}$ and BC concentrations were low (0.9–3.0 μg/m^3 and 0.06–0.27 μg/m^3, respectively), and the chemical composition was dominated by organic compounds and soot. The regional background concentrations increased as the weather got colder and the wind turned to blow from the east ($PM_{2.5}$: 3.3–7.6 μg/m^3, BC: 0.29–0.72 μg/m^3). During the eastern wind, the contribution of sulphate and ammonium increased in the particulate matter. A long-range transported (LRT) aerosol -episode on the 11th day contributed to high background particle concentrations and increased the nitrate levels that otherwise were very low. The yearly averaged $PM_{2.5}$ and BC in different measurement sites in the Helsinki metropolitan area were 4.6–6.3 μg/m^3 and 0.2–0.6 μg/m^3 in 2020, respectively (HSY, 2021). Thus, during the last three days of the campaign, the measured particle concentrations were closer to the typical concentrations in Helsinki than those measured in the beginning of the campaign.

In the residential area, the measured concentrations were close to the background concentrations during the days and warmer evenings. During the first measurement week, the average daytime $PM_{2.5}$ and BC in the residential area were 1.4 (standard deviation: 1.0–1.9) μg/m^3 and 0.46 (0.15–0.77) μg/m^3, and during the second week, 4.1 (2.9–5.3) μg/m^3 and 0.51 (0.22–0.79) μg/m^3, respectively. The residential wood combustion increased during the colder evenings, and the highest contribution of wood combustion was observed on the 5th day evening, when the average $PM_{2.5}$ and BC were 9.3 μg/m^3 and 2.40 μg/m^3, respectively. During the second week, the weather got colder, but stronger wind limited the contribution of combustion activities in the measured concentrations.

In the city centre, contribution of local traffic emissions was low due to the SARS-CoV-2-related partial lockdown. On the 2nd day, the average $PM_{2.5}$ and BC were 2.9 μg/m^3 and 0.47 μg/m^3, and on the 8th day 3.6 μg/m^3 and 0.49 μg/m^3, respectively. The measured concentrations were slightly higher in the driving measurements: The average concentrations on the 2nd and 8th day for $PM_{2.5}$ were 3.7 μg/m^3 and 6.6 μg/m^3, and for BC 1.25 μg/m^3 and 1.20 μg/m^3, respectively. Especially the measured $PM_{2.5}$ was lower than typically before the pandemic. For example, Luoma et al. (2021) reported long-term averaged $PM_{2.5}$ of 5.6–11.3 μg/m^3 and BC of 0.7–1.0 μg/m^3 at traffic sites in Helsinki before the pandemic.

Near the airport, the measured particle concentrations were low, except during aircraft take-offs, which caused significant peaks in the measured PN concentrations in Airport B, especially with particles smaller than 10 nm (Fig. 3, discussed in-detail in Section 3.2.3). Similar peaks were not detected with $PM_{2.5}$ or BC which were 5.0 and 0.84 μg/m^3 on average in Airport B, respectively. Airport A was further away from the runway 3 and, therefore, the number concentration peaks were not as evident although the PN concentrations increased occasionally. In Airport A, the average $PM_{2.5}$ and BC were 1.6 and 0.21 μg/m^3, respectively, which correspond well with the regional background concentrations during the measurements there (Table 1, Fig. 2).

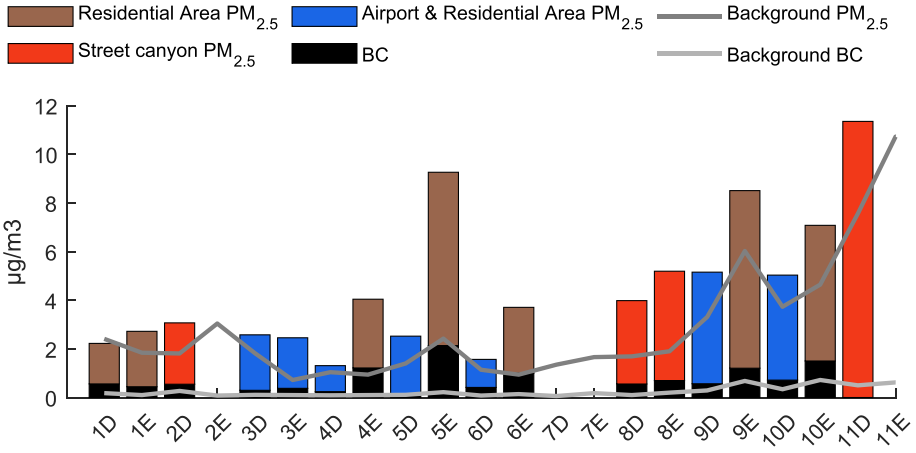

Fig. 2. The measured average $PM_{2.5}$ and BC concentrations during the measurement days (D: hours 8–17) and evenings (E: 17–22). The measurement locations during the day or evening are indicated with colours. Also, the regional background concentration levels (measured in the rural site in Luukki, Espoo) are shown. Measurements were not done in daytime on March 7th and during the evenings of March 2nd, 7th, and 11th. BC concentration was not measured on March 11th. During the other periods BC concentrations are included in the presented $PM_{2.5}$ concentrations.

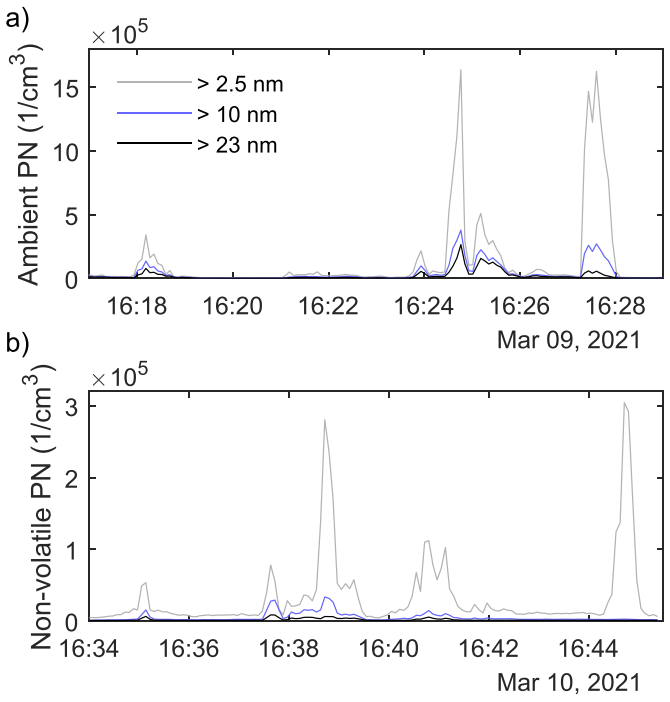

Fig. 3. Examples of a) ambient and b) non-volatile particle number (PN) concentration timeseries with different lower limits of the detected particle size in Airport B. Each PN concentration peak in the timeseries was measured directly after a plane take-off. Notice different scales on y-axes.

3.2. Fine particle characteristics, chemical composition, and morphology

3.2.1. Residential area

In the residential area, the highest contribution of the residential wood combustion was observed on the evenings of March 4th, 5th, and 6th, and, therefore, this section focuses on these days and evenings. During March 4th and 5th, the temperatures were cold, and the wind speed was moderate (Table 1). March 5th was Friday and 6th was Saturday, which are both traditional days to warm up saunas in Finland, which could contribute to the higher measured concentrations. Interestingly, there were notable differences in the particle characteristics during these evenings. Number size distributions of ambient and non-volatile particles during these evenings and the average from the day-time measurements are shown in Fig. 4. Also, the average measured concentrations are collected in Table 2.

As seen in Fig. 4 and Table 2, the average particle size profiles varied between the evenings. On the 4th evening, the contribution of both ambient and non-volatile particles smaller than 100 nm was higher, whereas on the other evenings, the relative fraction of soot mode particles around the size of 100 nm (and larger) increased. PN and NOx concentrations were higher on the 4th evening than on the other evenings whereas, on the 5th evening, the highest average $PM_{2.5}$ and BC were measured with a significant margin. High $PM_{2.5}$ and BC typically suggest contribution of residential wood combustion (Luoma et al., 2021, Saarikoski et al. 2021). The particle characteristics on the 6th evening were similar as on the 5th day except that the concentrations were lower.

The high PN and low mass concentrations on the 4th evening may suggest some other residential emission source, e.g., oil combustion. However, there were not significant differences in the chemical composition of particles between the 4th and 5th evenings as both were dominated with organics and biomass burning related BC (Fig. S1). According to the source apportionment analysis of organic aerosol (OA) (Fig. S3), biomass burning OA (BBOA) dominated OA composition during these evenings, constituting about 55% of total OA mass on both evenings. These results support the idea that the residential wood

Table 2
The average measured PN, PM, BC, and NOx concentrations in the residential area during March 4th – 6th. Also, 10th and 90th percentiles of the measured concentrations are shown in brackets. The number concentration of particles smaller than 23 nm were not determined on the 4th evening.

	4th Evening	5th Evening	6th Evening	4th – 6th Day
Ambient PN > 2.5 nm **(1/cm^3)**	–	16 600 (6800–33 300)	11 500 (9400–13 500)	8000 (5100–11 500)
Ambient PN > 10 nm **(1/cm^3)**	–	9000 (2900–20 400)	5700 (4300–6400)	3500 (1800–4800)
Ambient PN > 23 nm **(1/cm^3)**	12 700 (4100–24 200)	5900 (2300–11 600)	4400 (3500–5100)	2800 (1500–4000)
$PM_{2.5}$ **(μg/m^3)**	4.0 (2.2–7.2)	9.3 (2.5–15.0)	3.7 (2.6–5.0)	1.6 (1.1–2.8)
BC **(μg/m^3)**	1.22 (0.46–2.10)	2.40 (0.42–3.36)	1.19 (0.31–2.76)	0.29 (0.11–0.49)
NOx **(μg/m^3)**	26.3 (14.1–35.2)	16.0 (8.4–25.9)	16.8 (9.5–18.2)	10.0 (5.7–13.5)

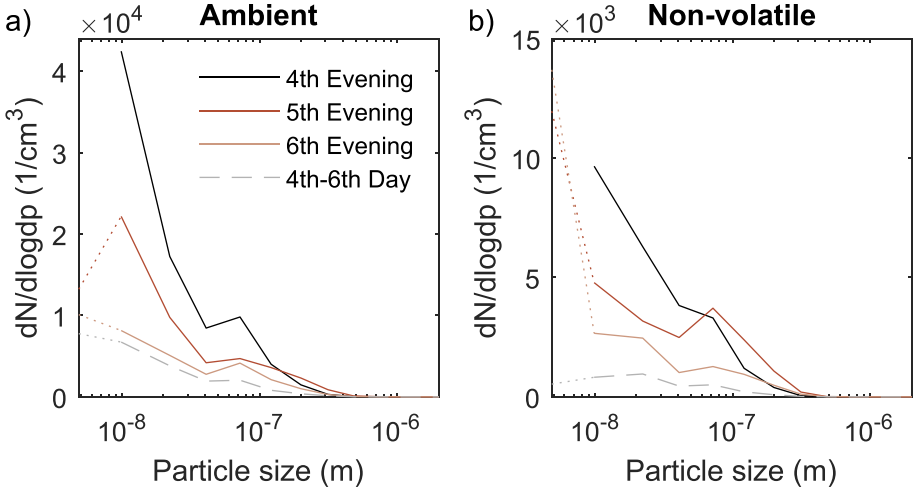

Fig. 4. The average a) ambient and b) non-volatile particle number size distributions measured in the residential area during March 4th – 6th. The dotted line below the size of 10^{-8} m represents CPC results. However, CPC results for the number size distributions were not determined on the 4th evening. The ambient and non-volatile particles were not measured simultaneously. Notice different scales on y-axes.

combustion was the dominant source of particles on both evenings (e.g., Harni et al., 2023). Interestingly, the contribution of hydrocarbon-like OA (HOA) was higher during the 5th evening (33%) than on the 4th evening (19%). This difference could be related e.g., to meteorological conditions or household solid waste combustion, which could increase the ultrafine particle emissions (Timonen et al. 2021). However, the low NOx concentration on the 5th evening excludes traffic as the source of the increased HOA. In general, the results on the 4th – 6th evenings indicate wood combustion as the main source of particles even though contribution of other residential sources cannot be fully excluded.

The results suggest that residential wood combustion is an important source of nanoparticles smaller than 23 nm. Especially with the non-volatile particles, a significant fraction of particles was observed to be smaller than 10 nm. This result indicates that primary emission particles from wood combustion can be very small even though wood combustion is usually considered to be a source of rather larger soot-mode particles and, thus, mainly a source of BC and $PM_{2.5}$ (e.g., Luoma et al., 2021; Saarikoski et al. 2021; Harni et al., 2023). Furthermore, previous studies considering primary emission particles smaller than 10 nm have mainly focused on combustion engines and traffic (e.g., Rönkkö et al., 2017). Thus, the results emphasize a gap of knowledge in the characteristics and sources of the smallest primary particles emitted by biomass combustion. Furthermore, the high fraction of sub 10 nm particles is an important observation in terms of the new WHO guidelines where the size range of ultrafine particles is not strictly defined (WHO, 2021). Also, the results during the 4th evening show that high concentration of ultrafine particles was not always connected with high BC and $PM_{2.5}$, highlighting that the contribution of the smallest ultrafine particles should not be forgotten when considering the monitoring of particulate emissions from residential sources. Unfortunately, there is no data of the smallest particle fraction during the 4th evening due to a CPC malfunction. Interestingly, in addition to the wood combustion, PN concentrations were clearly increased by the western wind during daytime on March 2nd and 3rd (Fig. S4), indicating that particle emissions from the airport or highway (Tuusulanväylä) may have contributed to increased PN during these days.

In the S/TEM analysis, the collected particles from residential area represented typical particle morphologies and elemental compositions related to wood combustion. For example, large (>0.5 μm) soot agglomerates and tar balls were found in the samples. In addition to elements which are always present in the samples (e.g., carbon and oxygen), particles containing potassium, silicon, and sulphur were regularly found in the samples (Fig. S5), which is typical with residential sources (Torvela et al., 2014; Pirjola et al., 2017). The comparison of S/TEM-sample results between the environments is discussed later and example samples are presented in Fig. 8.

3.2.2. Street canyon and city centre

The measured concentrations and particle number size distributions in the city centre (during 2nd and 8th of March) are shown in Fig. 5 and Table 3. On March 11th, a LRT-episode affected the concentrations significantly and, therefore, the results of March 11th are discussed later in Section 3.2.4. In general, the measured concentrations in the city centre were low in comparison with previous campaigns conducted in Helsinki (e.g., Hietikko et al., 2018; Lepistö et al., 2022), likely due to the lockdown and SARS-CoV-2 outbreak.

In ambient particle number size distributions, both nucleation and soot mode of particles were present as typically observed in traffic sites (e.g., Hietikko et al., 2018). The non-volatile particle size distributions consisted of particles smaller than 10 nm and soot agglomerates (20–200 nm) (see Rönkkö et al., 2014). Thus, the results in the street canyon represent rather typical characteristics of vehicle emissions. It should be noted that the majority of both ambient and non-volatile particles were smaller than 10 nm, indicating that most primary particle emissions from vehicular traffic are significantly smaller than 23 nm,

Table 3
The average PN, PM, BC, and NOx concentrations in the city centre on March 2nd and 8th. Also, 10th and 90th percentiles of the measured concentrations are shown in brackets.

	Street Canyon, 2nd March	Street Canyon, 8th March	Driving 2nd, March	Driving 8th, March
Ambient PN > 2.5 nm (1/cm^3)	43 600 (6600–107 400)	52 200 (19 800–91 300)	35 000 (5800–66 000)	65 300 (16 500–147 400)
Ambient PN > 10 nm (1/cm^3)	10 700 (2900–23 500)	15 000 (8300–22 100)	6400 (2500–13 800)	16 700 (7800–36 100)
Ambient PN > 23 nm (1/cm^3)	4300 (1700–7700)	5900 (3500–8800)	3900 (1800–6200)	7900 (4000–12 200)
$PM_{2.5}$ (μg/m^3)	2.9 (1.9–4.0)	3.6 (2.4–5.2)	3.7 (1.1–7.4)	6.6 (2.0–17.2)
BC (μg/m^3)	0.47 (0.14–0.93)	0.49 (0.25–0.80)	1.25 (0.19–2.86)	1.20 (0.35–2.06)
NOx (μg/m^3)	50 (18–93)	50 (18–104)	106 (23–207)	139 (40–272)

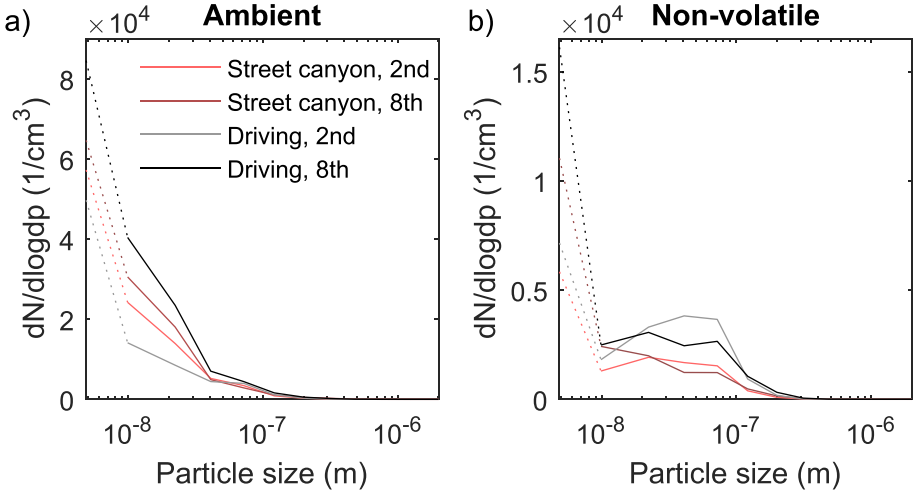

Fig. 5. The average a) ambient and b) non-volatile particle number size distributions measured in the city centre during March 2nd and 8th. The dotted line below the size of 10^{-8} m represents the CPC results. The ambient and non-volatile particles were not measured simultaneously. Notice different scales on y-axes.

which is the lower size limit used e.g., in the EURO emission standards. Also, when considering the WHO's statement for ultrafine particles, the measured PN concentrations in the city centre clearly exceeded the limits of high short-term (1-h average) PN concentration (20 000 1/cm^3), despite the reduced traffic rates due to the lockdown. In contrast, the measured $PM_{2.5}$ concentration was low and clearly below the WHO's recommendation (15 μg/m^3 for 24-h average). Thus, the elevated particle number emissions from road traffic were not well-observed with $PM_{2.5}$. Furthermore, in a recent study by Damayanti et al. (2023), it was observed that the concentrations of 7–30 nm particles from traffic have not decreased as clearly as the concentrations of particles larger than 30 nm during recent years. These observations highlight the importance of PN concentration monitoring in traffic sites in the future. Also, the observed high concentrations of sub 10 nm particles reveal the need to understand the trends with particles smaller than 7 nm which were not considered by Damayanti et al. (2023). In all, the results emphasize the fact that the selected lower limit of PN measurement size range has a major impact on the measured concentrations in traffic-influenced streets which should be considered in the future regulations and long-term studies.

There were not major differences between the stationary and driving measurements in the particle size distributions (Fig. 5), but the measured concentrations were slightly higher in the driving measurement than in the street canyon, except the PN on March 2nd. The higher concentrations during the driving measurements are likely explained with the shorter distance from tailpipes compared to the stationary measurement on the kerbside. Thus, the measurement results in the street canyon can be considered to represent the typical characteristics of particles in traffic-influenced streets of Helsinki city centre. The contribution of fossil fuel-originated BC was similar on both days. However, on March 8th, the contribution of organics and sulphates increased the total $PM_{2.5}$ concentration (Fig. S1). This difference is likely related to the weather conditions as, on March 8th, the temperature was colder and the wind speed was lower, indicating reduced dispersion of pollutants.

The S/TEM samples were dominated with soot agglomerates. The non-volatile particles smaller than 10 nm were very difficult to observe with the S/TEM which suggest carbonaceous composition as the TEM grid film material was carbon. However, with larger particles (>200 nm), various elements, e.g., aluminium, sodium, magnesium, potassium, chloride, phosphorus, sulphur, and calcium were found in the samples (Fig. S6-8). These elements may indicate some variation in the particle sources as potassium, calcium, phosphorus, and sulphur are found e.g., in diesel exhaust emissions (Kuuluvainen et al., 2020), whereas sodium, magnesium and chloride could be originated from the sea or road salt. Also, a C-rich tar-ball was found in the samples.

In addition to traffic, a coffee roastery near the street canyon (see e.g., Kuula et al., 2020) was observed to be a major source of ultrafine particles, and average PN of particles larger than 2.5 nm, 10 nm and 23 nm of a plume originated from the roastery were 27 800, 15 400 and 13 000 1/cm^3, respectively (additional results in Fig. S9-11). This result shows that air quality near similar non-regulated local sources can be poor. It is likely that the relative contribution of similar sources will increase in the future as the emission control of vehicles and other sources improve. The example with the coffee roastery shows the importance of dense air quality monitoring in cities to recognize the contribution of local individual sources on urban air quality.

3.2.3. Airport

As seen in Fig. 3, departing aircrafts caused significant increases in PN outside the airport, especially in the second measurement location (Airport B). As Airport B can be considered to represent emissions from aircrafts more clearly, the focus in this section is on the results from Airport B. The measured particle number size distributions and concentrations measured in Airport B are shown and compared with the other studied environments in Figs. 6 and 7. The average concentrations in Airport B are collected in Table 4. The compared results from the residential area and the street canyon in Figs. 6 and 7 are selected from periods which represented the contribution of the local emissions the clearest. In the residential area, the chosen period was the 5th evening

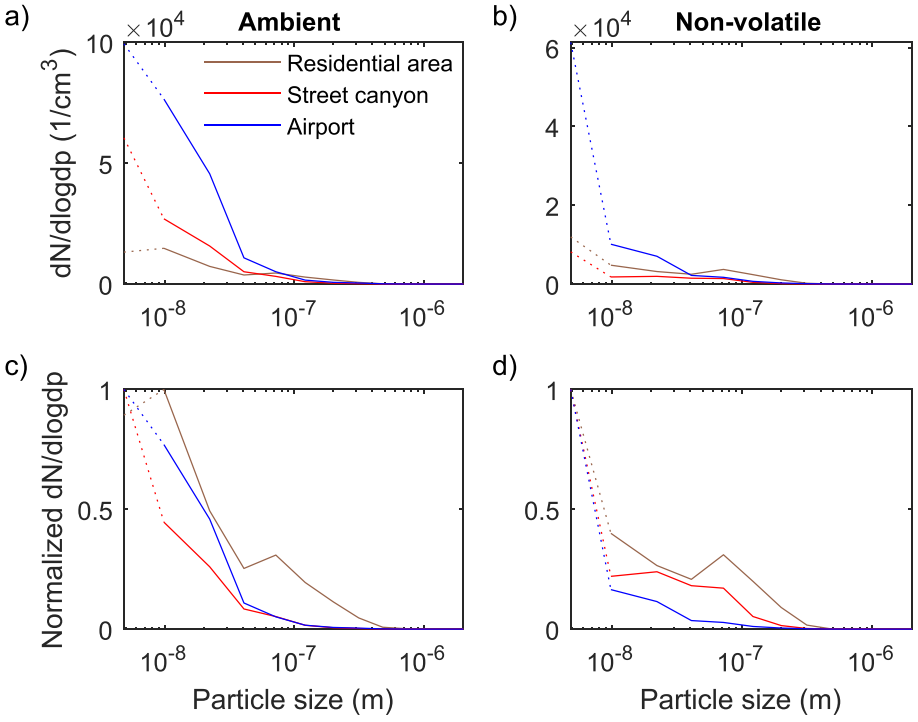

Fig. 6. The average a) ambient, and b) non-volatile particle number size distributions during the chosen representative periods of the studied environments. Also, normalized c) ambient, and d) non-volatile particle number size distributions are shown. The dotted line below the size of 10^{-8} m represents the CPC results. The ambient and non-volatile particles were not measured simultaneously. Notice different scales on y-axes.

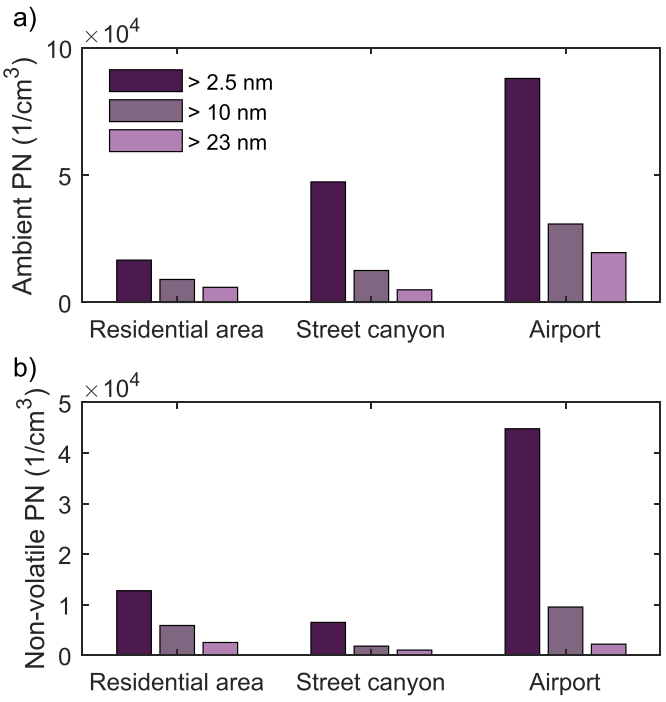

Fig. 7. The average a) ambient, and b) non-volatile particle number (PN) concentrations with three different lower limits of the detectable size range during the chosen representative periods of the studied environments. The ambient and non-volatile particles were not measured simultaneously. Notice different scales on y-axes.

while, in the street canyon, the data from both 2nd and 8th day was chosen. Additionally, results from Airport A are provided in Supplementary (Fig. S12-14).

In Figs. 3, 6 and 7, particle emissions from aircrafts were clearly dominated by ultrafine particles smaller than 50 nm, most particles being smaller than 10 nm. A major contribution to PN can especially be seen when comparing the airport with the other environments. In the street canyon, the relative fraction of ambient particles smaller than 10 nm was rather similar as in the airport. However, with the non-volatile particles, the relative fraction of sub 10 nm particles in the airport was significant in comparison with the street canyon, emphasizing the air traffic as a source of the smallest ultrafine particles. On the other hand, the relative fraction of soot mode particles near the airport was smaller than in the other environments. It should be mentioned that the high number of particles smaller than 10 nm were not detected only in Airport B as similar particle characteristics were also observed in Airport A (Fig. S12-14).

Despite the high ultrafine particle concentrations, the average $PM_{2.5}$ and BC concentrations during the measurements in Airport B were low (Table 4: 5.0 and 0.84 μg/m^3, respectively). By taking the regional background ($PM_{2.5}$: 3–4 μg/m^3 and BC: 0.3–0.4 μg/m^3) into account, the results suggest that the air traffic was not a major source of $PM_{2.5}$ or BC. This result is supported with the particle number size distributions and the SP-AMS which did not observe any mass concentration peaks near the airport due to the small particle size. The results near the airport suggest that the high PN concentrations measured in the residential area during the western wind (Fig. S4) could be originated from the airport (see also Hudda et al. 2014 and Keuken et al., 2015), emphasizing the role of air traffic in urban air quality even far away from the airport. The major ultrafine particle emissions from aircrafts have been observed in previous studies, but the lower limits of the measurement size ranges have typically been larger than 2.5 nm (Stacey, 2019). Thus, according to our results, despite that the air traffic has been known to be a major emission source of ultrafine particles, a significant fraction of these particles are in previously unobserved size ranges, emphasizing the need to study nanocluster aerosol emissions of aviation. Furthermore, these high ultrafine particle concentrations are not easily detected with particle mass measurement and the emissions can increase the PN concentrations clearly above the WHO's suggested limit for high short-term PN (20 000 1/cm^3). The results emphasize the need for long-term measurements of ultrafine particles, especially the sub 10 nm fraction, near airports, and highlight the importance of the chosen lower limit of PN measurement size range, which should be recognized e.g., in the future regulations.

Examples of the S/TEM images of the samples from Airport B, including the other studied environments, are shown in Fig. 8. The samples from the airport suggest that the non-volatile sub 10 nm particles were carbonaceous as they were difficult to observe with the S/

Table 4
The average PN, PM, BC, and NOx concentrations in Airport B. Also, 10th and 90th percentiles of the measured concentrations are shown in brackets.

	Airport B
Ambient PN > 2.5 nm **(1/cm^3)**	88 000 (6700–299 000)
Ambient PN > 10 nm **(1/cm^3)**	30 800 (3400–94 800)
Ambient PN > 23 nm **(1/cm^3)**	19 600 (2600–56 300)
$PM_{2.5}$ **(μg/m^3)**	5.0 (1.6–7.6)
BC **(μg/m^3)**	0.84 (0.27–1.06)
NOx **(μg/m^3)**	30.2 (12.4–45.0)

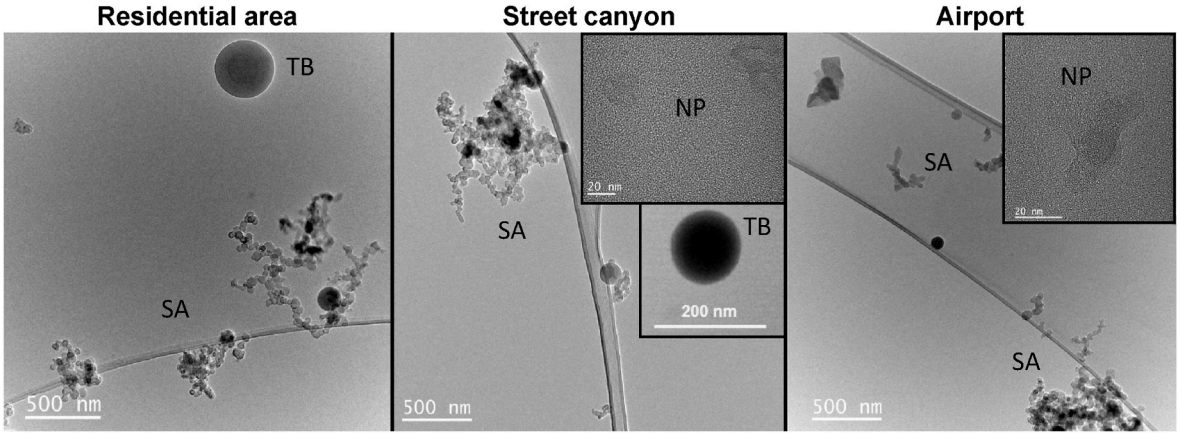

Fig. 8. Example S/TEM images of collected soot agglomerates (SA) in all the studied environments. Also, C-rich tar-balls (TB) can be seen in the samples from the residential area and the street canyon. Furthermore, examples of barely observable approximately 20 nm carbonaceous nanoparticles (NP) are shown in the samples from the street canyon and the airport.

TEM, similarly as in the street canyon. Again, a significant fraction of soot agglomerates was found in the samples. However, in comparison with the other environments, there seemed to be more variability in the elemental composition of particles: Various elements, e.g., aluminium, zinc, iron, titanium, sodium, magnesium, sulphur, and potassium were found (Fig. S15-16). These elements were mainly found in particles larger than 100 nm. Especially aluminium, zinc, iron, sodium, magnesium, and titanium have been associated with aircraft exhaust before (Abegglen et al., 2016; Turgut et al., 2019).

The estimated emissions factors for PN, PM, BC, and NOx in the street canyon and near the airport are collected in Supplementary (Table S2). In general, the estimated emission factors in the street canyon were lower than in previous studies conducted in Helsinki (Enroth et al., 2016; Hietikko et al., 2018). The decreased emission factors may indicate that the vehicular emission regulations have improved the urban air quality over the years. Near the airport, all the estimated emission factors were significantly higher than in the street canyon. Especially, the PN emission factors were approximately 10–100 times higher in the airport. According to previous studies (e.g., Lobo et al., 2012; Schripp et al., 2018) and the results (Fig. S17), the emission factors depend on the plane type, emphasizing the importance and need for emission regulating technologies with aircrafts. Interestingly, in the residential area, it was observed that the emission ratio of non-volatile PN as a function of CO_2 (with PN > 10 nm: 314 1/cm^{3}ppm) was higher than, in the street canyon (114 1/cm^{3}ppm), highlighting the wood combustion as a source of ultrafine particles.

3.2.4. LRT-episode

On March 11th, air masses originating from Baltics and Poland (Fig. S19) caused a LRT-episode, which clearly increased the background $PM_{2.5}$ (Fig. 2). In particle size distributions, the LRT-episode was seen with the accumulation mode particles (Fig. S20-21). Furthermore, concentrations of nitrates, sulphates and ammonium increased during the LRT-episode (Fig. S1). However, the LRT-episode was not observed with ambient PN: In the street canyon, the average concentration of particles larger than 2.5 nm, 10 nm and 23 nm on March 11th were 37 500, 8000 and 3500 1/cm^3, respectively. These concentrations are lower than the concentrations measured during the 2nd and 8th day in the street canyon (Table 3). However, the concentration of non-volatile particles smaller than 50 nm increased notably during the LRT-episode, which suggest that even the smaller ultrafine particles can transport to far distances (Fig. S21). On the other hand, the average $PM_{2.5}$ during March 11th in the street canyon was 10.4 μg/m^3 which is over three times higher than on March 2nd or 8th. Therefore, even though the road traffic was a major source of ultrafine particles, $PM_{2.5}$ in the city centre was clearly more depended on the regional background aerosol than on the traffic. Similar observations can be seen in the other studied urban environments as well even though residential wood combustion increased also $PM_{2.5}$. Thus, $PM_{2.5}$ does not indicate well the ultrafine particle concentrations in cities, emphasizing the need for PN concentration monitoring in different urban environments when considering the effects of local emission sources on public health.

3.3. Particle respiratory tract deposition

In section 3.2., it was observed that the urban aerosol characteristics varied significantly in each of the studied locations and the contribution of the site-describing pollution source (wood combustion, traffic, aviation) was clear. The varying aerosol characteristics may be crucial in terms of particle exposure and possible health impacts. For example, the differences in the particle sizes lead to different particle deposition efficiencies in the human respiratory tract and, therefore, different lung exposure of pollutants. In addition, the results indicate different chemistry of the inhaled particles, which suggests varying toxicity and health impacts. In this study, LDSA was used as a tracer of the potential health effects related to particulate exposure. The comparison of LDSA size distributions and concentrations are shown in Fig. 9 and Table 5. Also, the relationships between LDSA and the other studied particle metrics (PN, $PM_{2.5}$, BC) based on the average concentrations are shown in Table 5. The compared measurement periods in Fig. 9 and Table 5 are the same as in the previous comparison in Figs. 6 and 7. Additionally, the data from the urban background site during the LRT-episode (11th March) was chosen to represent the contribution of the LRT aerosol.

As seen in Fig. 9, the peak sizes of the LDSA size distributions varied notably in the studied environments. Near the airport, the size distribution was at the highest around the size of 20 nm and the majority of LDSA was caused by particles smaller than 100 nm which can be seen also in Table 5 as a high deviation of LDSA caused by sub 55 nm particles. The major contribution of the smallest ultrafine particles to LDSA is an important observation as LDSA has usually been linked to soot or accumulation mode particles near size 100 nm (e.g., Lepistö et al., 2022; Teinilä et al., 2022). 100 nm is also the size which is usually utilized in the calibration of the sensor-based LDSA measurement (e.g., Fissan et al., 2006; Fierz et al., 2014) and, thus, the result indicates that accuracy of the sensor-based LDSA measurement may decrease near airports. In the street canyon, the contribution of sub 55 nm particles was high as well but the relative contribution of 50 nm–100 nm particles was notably higher there than near the airport. The LDSA size distributions in the street canyon agreed with previous studies (e.g., Kuuluvainen et al., 2016; Pirjola et al., 2017; Lepistö et al., 2022), but the fraction of particles smaller than 100 nm was higher in this study, which emphasizes the role of ultrafine particles, along with BC, in LDSA near road traffic. The differences between the studies may relate to the winter conditions and reduced traffic rates. In the residential area, the LDSA size distribution differed significantly in comparison with the street canyon and the airport, and the distribution was dominated by 50–400 nm particles. Furthermore, during the LRT-episode, the LDSA was dominated by 200–700 nm particles. These differences highlight the need to consider particle sizes in LDSA measurements as the accuracy of the typical LDSA sensors may decrease with larger particles.

The results in Fig. 9 suggest that the characteristics of lung-depositing particles depend significantly on the urban environment in Finland. Also, the varying particle sizes contributing to LDSA along the varying conditions and regional background $PM_{2.5}$ affect the relationship between LDSA and the other studied metrics. Near the airport, LDSA per unit $PM_{2.5}$ was 1.4 and 2.4 times higher than in the street canyon and the residential area, respectively, whereas, during the LRT-episode, LDSA per unit $PM_{2.5}$ decreased significantly. The results suggest that $PM_{2.5}$ does not indicate the LDSA concentration caused by nearby pollution sources and ultrafine particles well. On the other hand, LDSA per unit PN in the residential area was 5.0 and 4.2 times higher than in the street canyon and the airport, respectively. Also, the connection between LDSA and BC varied between the environments. However, it should be noted that, in the street canyon, the ratio between LDSA and BC was notably higher than in previous studies conducted in the same street canyon (7.7–13.5 mm^2/gμ, Kuula et al., 2020; Lepistö et al., 2022), which is likely explained with the very low BC concentration. In the residential area, the ratio between BC and LDSA was close to 8.4 mm^2/μg, which is reported from another residential area by Kuula et al. (2020).

The varying particle characteristics and the connections between LDSA and the widely measured $PM_{2.5}$ suggest that the health effects related to $PM_{2.5}$ are depended on the location and the dominating emission source since the lung deposition of particles per unit $PM_{2.5}$ is not constant and depends on regional background aerosol. The limitations of $PM_{2.5}$ can be emphasized also by normalizing the measured PN, LDSA, and BC concentrations based on $PM_{2.5}$ (Table S3). For example, in the street canyon, average PN (>2.5 nm) per cubic centimetre was approximately 2.9 higher than in the residential area, whereas PN per particle mass ($PM_{2.5}$) was over 8 times higher. Thus, by focusing only on $PM_{2.5}$ in monitoring measurements, the effects of ultrafine particles from different emission sources may be missed. For example, it has been

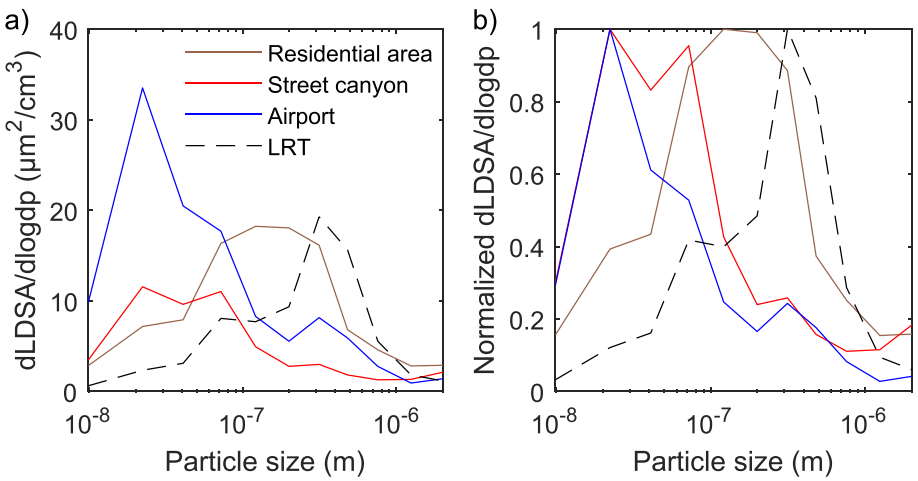

Fig. 9. The a) average and b) normalized LDSA size distributions during the chosen representative periods of the studied environments and during the LRT-episode.

Table 5
The average LDSA, PN > 2.5 nm, $PM_{2.5}$, BC concentrations, including 10th and 90th percentiles, during the chosen representative periods of the studied environment and during the LRT-episode (only average). Also, the size dependency of LDSA and the relationship with PN, $PM_{2.5}$ and BC concentrations is shown.

Location	LDSA (μm²/cm³)	LDSA <55 nm (μm²/cm³)	LDSA 55–260 nm (μm²/cm³)	LDSA >260 nm (μm²/cm³)	PN > 2.5 nm (1/cm³)	$PM_{2.5}$ (μg/m³)	BC (μg/m³)	LDSA/PN (>2.5 nm) (μm²)	LDSA/$PM_{2.5}$ (mm²/μg)	LDSA/BC (mm²/μg)
Residential area	22.6 (6.9–34.2)	5.1 (1.7–12.1)	11.5 (3.1–19.4)	6.0 (1.2–17.6)	16 600 (6800–33 300)	9.3 (2.5–15.0)	2.40 (0.42–3.36)	$14*10^{-4}$	2.4	9.4
Street canyon	13.2 (5.8–21.8)	7.1 (2.3–13.6)	4.3 (2.1–7.2)	1.8 (1.0–2.6)	47 400 (9300–102 900)	3.2 (2.1–4.7)	0.43 (0.16–0.77)	$2.8*10^{-4}$	4.1	30.7
Airport	29.2 (7.9–73.5)	18.6 (2.4–56.1)	7.1 (2.9–11.8)	3.5 (2.3–6.0)	88 000 (6700–299 000)	5.0 (1.6–7.6)	0.84 (0.27–1.06)	$3.3*10^{-4}$	5.8	34.8
LRT	15.4	1.7	5.6	8.1	5000	10.1	–	$31*10^{-4}$	1.5	–

suggested that the negative health effects per unit $PM_{2.5}$ increase near local ultrafine particle sources e.g., traffic (Segersson et al., 2021). Thus, according to the results, increased lung deposition and LDSA per unit $PM_{2.5}$ due to ultrafine particles may have an important role in the results of epidemiological studies. However, LDSA's relationships with both BC and PN were also heavily depended on the location, emphasizing the need to understand how different metrics in general relate to the health effects in different environments.

It should be noted that the results in Fig. 9 and Table 5 are based on short measurements periods during certain conditions. Especially the effect of weather conditions and seasonality should be mentioned. For example, residential wood combustion is common only during colder evenings of winter. Also, LDSA in the street canyon (13.2 $\mu m^2/cm^3$) was notably lower than in August 2019 in the same street canyon (27.2 $\mu m^2/cm^3$, Lepistö et al., 2022). Thus, differences between winter and summer may be important when considering e.g., the effects of photochemistry, condensation, as well as dispersion of pollutants even though SARS-CoV-2 may also have affected the reduced LDSA in the latter example. Thus, long-term studies of the connection between LDSA and other metrics would be beneficial to understand the main causes of particle lung deposition, and possible health effects in different environments better.

In all, the results with LDSA highlight the importance of monitoring the ultrafine particle concentrations in cities, especially near airports and road traffic. On the other hand, $PM_{2.5}$ and BC are also important metrics especially in residential areas and with regional background aerosol. However, it should be noted that LDSA considers only the alveolar particle deposition and, therefore, it does not cover and explain all the health effects caused by ambient fine particles. For example, it is likely that particle deposition in the other respiratory tract regions causes adverse health effects as well. As seen in Section 3.2, significant fraction of particles in all the studied environments were smaller than 10 nm. According to ICRP (1994) model, approximately 15–50% of particles with sizes from 2.5 nm to 10 nm deposit in the head airways, depending on particle size. As mentioned in Introduction, studies have suggested that particles could enter the human brain directly from head airways via the olfactory nerve. Thus, high concentrations of sub 10 nm particles, especially in the airport and street canyon, indicate a major risk of particle exposure in the human brain. Therefore, in urban areas, which are near pollution sources emitting nanoparticles (e.g., traffic), the risk for adverse brain effects caused by particle emissions could be high. Furthermore, the observed high concentrations of non-volatile particles below the size of 10 nm in all the environments could be related to the toxicity of particles that end up inside the human body. For example, it has been observed that 5 nm primary particles may translocate from the lungs to urine more efficiently than 30 nm particles (Miller et al., 2017). However, the health effects caused by both, particles smaller than 10 nm and the non-volatile particles, are still poorly understood, and therefore, conclusions about the health impacts cannot be made. Thus, the results emphasize the need for toxicological and epidemiological studies to understand the role of ultrafine particles in the health burden caused by ambient fine particles.

4. Conclusions

In this study, wintertime physical and chemical characteristics of urban air fine particles were investigated in a detached housing area with residential wood combustion, traffic-influenced streets in the city

centre and near an airport. It was found that there are significant differences e.g., in the particle sizes, volatility and chemical composition in the studied environments. In addition, a long-range transported aerosol (LRT) event affecting the measured aerosol concentrations and composition was observed during the measurements.

In the residential area, the contribution of evening-time wood combustion was observed as increased BC and $PM_{2.5}$, which was expected. However, residential wood combustion was also a source of ultrafine particles smaller than 10 nm and 23 nm. In the city centre, the measured $PM_{2.5}$ and BC were low due to SARS-CoV-2-related partial lockdown, which reduced the traffic rates. Despite the lockdown, the ultrafine particle concentrations still exceeded the WHO's definition for high PN concentration (1-h average $>$ 20 000 1/cm^3). Near the airport, departing aircrafts caused significant peaks in PN concentration, and WHO's definition for high concentration was clearly exceeded. However, these elevated concentrations were not detected well with BC or $PM_{2.5}$, which emphasizes the role of air traffic as a source of ultrafine particles, but not as a major source of particle mass. In both, the city centre and near the airport, majority of the observed ambient and non-volatile particles were smaller than 10 nm. These results may indicate underestimation of the health effects caused by the studied sources in previous studies based on particle mass measurement.

The observed differences in the particle characteristics suggest different human exposure in the studied environments. Near the airport, lung deposited surface area (LDSA) size distribution was dominated by particles smaller than 50 nm, in the city centre by particles between 20 nm and 100 nm, and in the residential area by particles with sizes from 50 nm to 400 nm. During the LRT-episode, LDSA was dominated with even larger particles (200 nm–700 nm). These results suggest major differences in the composition of the lung-depositing particles, indicating different health impacts of particle exposure. Furthermore, the observed differences in particle chemical and elemental composition in the studied environments have likely effects on the toxicity of particles as well. Also, the high concentrations of sub 10 nm particles could indicate increased risk of particle exposure in the human brain.

The results of this study emphasize the need of various metrics in urban fine particle monitoring and regulations in addition to $PM_{2.5}$. For example, near the airport and in the city centre, high ultrafine particle concentrations did not correlate well with $PM_{2.5}$ and BC. In the residential area, wood combustion contributed to $PM_{2.5}$ and BC as well, but throughout the campaign $PM_{2.5}$ was the most depended on the regional background concentration and the LRT-aerosol. On the other hand, the LRT-episode was not observable with PN concentration. Thus, there may be major differences in health effects caused by local and distant sources per unit $PM_{2.5}$. Also, it is likely that the health impacts relating to the different particle metrics depend notably on the urban environment and the conditions. For example, due to the major ultrafine particle emissions, LDSA per unit $PM_{2.5}$ in the airport was 1.4 and 2.4 times higher than in the street canyon and the residential area, respectively. Also, even though the LRT-episode contributed to high $PM_{2.5}$, the role in the LDSA was low compared to the local sources. Furthermore, the results show the importance of the chosen lower limit of the particle size range when measuring the number concentration of ultrafine particles. In the WHO's guidelines, it is stated that the lower limit should be 10 nm or smaller. However, especially near the airport and in the city centre, most particles were smaller than 10 nm, showing that the chosen lower limit significantly affects the measured concentrations.

Due to the relatively short measurement campaign and varying conditions, the measured concentrations of this study should not be generalized as long-term averages as the results represent the particle characteristics only during certain situations and conditions. However, the results emphasize the effects of local emission sources in terms of urban air quality and the need to understand how these sources affect human health. Furthermore, the health impacts relating to particles smaller than 10 nm are still poorly understood even though, according to this study, majority of urban air particles are smaller than 10 nm. In all, there is a need for long-term measurements in various urban environments to properly understand the average human exposure as a function of different metrics, and how these metrics are connected to the human health.

Credit author statement

T. Lepistö: Conceptualization; Data curation; Formal analysis; Investigation; Methodology; Validation; Visualization; Writing - original draft; Writing - review & editing.L.M.F. Barreira: Data curation; Formal analysis; Investigation; Validation; Visualization; Writing - original draft; Writing - review & editing.A. Helin: Investigation; Writing – review & editing.J.V. Niemi: Methodology; Resources; Writing - review & editing.N. Kuittinen: Investigation; Project administration; Writing - review & editing.H. Lintusaari: Methodology; Visualization; Writing - review & editing.V. Silvonen: Investigation; Writing – review & editing. L. Markkula: Investigation; Writing – review & editing.H.E. Manninen: Resources; Writing – review & editing.H. Timonen: Funding acquisition; Methodology; Project administration; Writing - review & editing.P. Jalava: Funding acquisition; Project administration; Supervision; Writing - review & editing.S. Saarikoski: Funding acquisition; Investigation; Methodology; Project administration; Writing - review & editing. T. Rönkkö: Conceptualization; Funding acquisition; Methodology; Project administration; Supervision; Writing - review & editing.

Declaration of competing interest

The authors declare that they have no known competing financial interests or personal relationships that could have appeared to influence the work reported in this paper.

Data availability

Data will be made available on request.

Acknowledgements

This work is part of the European Union's Horizon 2020 research and innovation programme under grant agreement No 814978 (TUBE: Transport-derived ultrafines and the brain effects).

This work has received funding from BC Footprint project (530/31/2019) funded by Business Finland, participating companies and municipal actors.

We gratefully acknowledge Academy of Finland Flagship funding Atmosphere and Climate Competence Centre, ACCC (grant no. 337552, 337551).

Teemu Lepistö thanks Finnish Foundation for Technology Promotion for supportive funding for the doctoral studies.

We wish to thank Tampere Microscopy Centre for the analysis of S/TEM and EDS samples as well as HSY's measurement team and Stanislav Demyanenko for their valuable work during the measurement campaign.

The authors gratefully acknowledge the NOAA Air Resources Laboratory (ARL) for the provision of the HYSPLIT transport and dispersion model and READY website (https://www.ready.noaa.gov) used in this publication.

Appendix A. Supplementary data

Supplementary data to this article can be found online at https://doi.org/10.1016/j.envres.2023.116068.

References

Abegglen, M., Brem, B.T., Ellenrieder, M., Durdina, L., Rindlisbacher, T., Wang, J., Lohmann, U., Sierau, B., 2016. Chemical characterization of freshly emitted

particulate matter from aircraft exhaust using single particle mass spectrometry. Atmos. Environ. 134, 181–197. https://doi.org/10.1016/j.atmosenv.2016.03.051.
Aguilera, I., Dratva, J., Caviezel, S., Burdet, L., de Groot, E., Ducret-Stich, R.E., Eeftens, M., Keidel, D., Meier, R., Perez, L., Rothe, T., Schaffner, E., Schmit-Trucksäss, A., Tsai, M.Y., Schindler, C., Künzli, N., Probst-Hensch, N., 2016. Particulate matter and subclinical atherosclerosis: associations between different particle sizes and sources with carotid intima-media thickness in the SAPALDIA study. Environ. Health Perspect. 124, 1700–1706. https://doi.org/10.1289/EHP161.
Amanatidis, S., Ntziachristos, L., Karjalainen, P., Saukko, E., Simonen, P., Kuittinen, N., Aakko-Saksa, P., Timonen, H., Rönkkö, T., Keskinen, J., 2018. Comparative performance of a thermal denuder and a catalytic stripper in sampling laboratory and marine exhaust aerosols. Aerosol. Sci. Technol. 52 (4), 420–432. https://doi.org/10.1080/02786826.2017.1422236.
Barreira, L.M.F., Helin, A., Aurela, M., Teinilä, K., Friman, M., Kangas, L., Niemi, J.V., Portin, H., Kousa, A., Pirjola, L., Rönkkö, T., Saarikoski, S., Timonen, H., 2021. In-depth characterization of submicron particulate matter inter-annual variations at a street canyon site in northern Europe. Atmos. Chem. Phys. 21, 6297–6314. https://doi.org/10.5194/acp-21-6297-2021.
Brown, D.M., Wilson, M.R., MacNee, W., Stone, V., Donaldson, K., 2001. Size-dependent proinflammatory effects of ultrafine polystyrene particles: a role for surface area and oxidative stress in the enhanced activity of ultrafines. Toxicol. Appl. Pharmacol. 175 (3), 191–199. https://doi.org/10.1006/taap.2001.9240.
Burnett, R.T., Pope, C.I.I., Ezzati, M., Olives, C., Lim, S.S., Mehta, S., Shin, H.H., Singh, G., Hubbell, B., Brauer, M., et al., 2014. An integrated risk function for estimating the global burden of disease attributable to ambient fine particulate matter exposure. Environ. Health Perspect. 122 (4), 397–403. https://doi.org/10.1289/ehp.1307049.
Canagaratna, M.R., Jayne, J.T., Jimenez, J.L., Allan, J.D., Alfarra, M.R., Zhang, Q., Onasch, T.B., Drewnick, F., Coe, H., Middlebrook, A., et al., 2007. Chemical and Microphysical Characterization of Ambient Aerosols with the Aerodyne Aerosol Mass Spectrometer, vol. 26, pp. 185–222. https://doi.org/10.1002/mas.20115.
Carbone, S., Aurela, M., Saarnio, K., Saarikoski, S., Timonen, H., Frey, A., Sueper, D., Ulbrich, I.M., Jimenez, J.L., Kulmala, M., et al., 2014. Wintertime aerosol chemistry in Sub-arctic urban air. Aerosol Sci. Technol. 48 (3), 313–323. https://doi.org/10.1080/02786826.2013.875115.
Cassee, F.R., Héroux, M.-E., Gerlofs-Nijland, M.E., Kelly, F.J., 2013. Particulate matter beyond mass: recent health evidence on the role of fractions, chemical constituents and sources of emission. Inhal. Toxicol. 25 (14), 802–812. https://doi.org/10.3109/08958378.2013.850127.
Cohen, A.J., Brauer, M., Burnett, R., Anderson, H.R., Frostad, J., Estep, K., Balakrishnan, K., Brunekreef, B., Dandona, L., Dandona, R., et al., 2017. Estimates and 25-year trends of the global burden of disease attributable to ambient air pollution: an analysis of data from the Global Burden of Diseases Study 2015. Lancet 389 (10082), 1907–1918. https://doi.org/10.1016/S0140-6736(17)30505-6.
Damayanti, S., Harrison, R.M., Pope, F., Beddows, D.C.S., 2023. Limited impact of diesel particle filters on road traffic emissions of ultrafine particles. Environ. Int. 174 https://doi.org/10.1016/j.envint.2023.107888.
Dockery, D.W., Pope, C.A., Xu, X., Spengler, J.D., Ware, J.H., Fay, M.E., Ferris Jr., B.G., Speizer, F.E., 1993. An association between air pollution and mortality in six U.S. cities. N. Engl. J. Med. 329 (24), 1753–1759. https://doi.org/10.1056/NEJM199312093292401.
Drinovec, L., Močnik, G., Zotter, P., Prévôt, A.S.H., Ruckstuhl, C., Coz, E., Rupakheti, M., Sciare, J., Müller, T., Wiedensohler, A., Hansen, A.D.A., 2015. The "dual-spot" Aethalometer: an improved measurement of aerosol black carbon with real-time loading compensation. Atmos. Meas. Tech. 8, 1965–1979. https://doi.org/10.5194/amt-8-1965-2015.
Enroth, J., Saarikoski, S., Niemi, J., Kousa, A., Ježek, I., Močnik, G., Carbone, S., Kuuluvainen, H., Rönkkö, T., Hillamo, R., Pirjola, L., 2016. Chemical and physical characterization of traffic particles in four different highway environments in the Helsinki metropolitan area. Atmos. Chem. Phys. 16, 5497–5512. https://doi.org/10.5194/acp-16-5497-2016.
European Environment Agency, 2021. Air Quality in Europe - 2021 Report. https://doi.org/10.2800/549289.
Fierz, M., Meier, D., Steigmeier, P., Burtscher, H., 2014. Aerosol measurement by induced currents. Aerosol. Sci. Technol. 48 (4), 350–357. https://doi.org/10.1080/02786826.2013.875981.
Fissan, H., Neumann, S., Trampe, A., Pui, D., Shin, W., 2006. Rationale and principle of an instrument measuring lung deposited nanoparticle surface area. J. Nanoparticle Res. 9 (1) https://doi.org/10.1007/978-1-4020-5859-2_6, 53–9.
Gemmer, M., Xiao, B., 2013. Air quality legislation and standards in the European union: background, status and public participation. Adv. Clim. Change Res. 4 (1), 50–59. https://doi.org/10.3724/SP.J.1248.2013.050.
Harni, S.D., Saarikoski, S., Kuula, J., Helin, A., Aurela, M., Niemi, J.V., Kousa, A., Rönkkö, T., Timonen, H., 2023. Effects of Emission Sources on the Particle Number Size Distribution of Ambient Air in the Residential Area. Atmospheric Environment. https://doi.org/10.1016/j.atmosenv.2022.119419.
Heikkilä, J., Virtanen, A., Rönkkö, T., Keskinen, J., Aakko-Saksa, P., Murtonen, T., 2009. Environ. Sci. Technol. 43 (24), 9501–9506. https://doi.org/10.1021/es9013807.
Helin, A., Niemi, J.V., Virkkula, A., Pirjola, L., Teinilä, K., Backman, J., Aurela, M., Saarikoski, S., Rönkkö, T., Asmi, E., Timonen, H., 2018. Characteristics and source apportionment of black carbon in the Helsinki metropolitan area, Finland. Atmos. Environ. 190, 87–98. https://doi.org/10.1016/j.atmosenv.2018.07.022.
Helin, A., Virkkula, A., Backman, J., Pirjola, L., Sippula, O., Aakko-Saksa, P., Väätäinen, S., Mylläri, F., Järvinen, A., Bloss, M., Aurela, M., Jakobi, G., Karjalainen, P., Zimmermann, R., Jokiniemi, J., Saarikoski, S., Tissari, J., Rönkkö, T., Niemi, J.V., Timonen, H., 2021. Variation of absorption Ångström exponent in aerosols from different emission sources. J. Geophys. Res. Atmos. 126, e2020JD034094 https://doi.org/10.1029/2020JD034094.
Hennig, F., Quass, U., Hellack, B., Küpper, M., Kuhlbusch, T.A.J., Stafoggia, M., Hoffmann, B., 2018. Ultrafine and fine particle number and surface area concentrations and daily cause-specific mortality in the ruhr area. Germany Environ. Health Perspect. 126 (2 CID), 027008. https://doi.org/10.1289/EHP2054, 2009–2014.
Hietikko, R., Kuuluvainen, H., Harrison, R.M., Portin, H., Timonen, H., Niemi, J.V., Rönkkö, T., 2018. Diurnal variation of nanocluster aerosol concentrations and emission factors in a street canyon. Atmos. Environ. 189, 98–106. https://doi.org/10.1016/j.atmosenv.2018.06.031.
HSY (Helsinki Region Environmental Services Authority), 2021. Ilmanlaatu Pääkaupunkiseudulla Vuonna 2020 – Vuosiraportti (Air Quality in Helsinki Metropolitan Area in 2020 – Annual Report).
Hudda, N., Gould, T., Hartin, K., Larson, T.V., Fruin, S.A., 2014. Emissions from an international airport increase particle number concentrations 4-fold at 10 km downwind. Environ. Sci. Technol. 48 (12), 6628–6635. https://doi.org/10.1021/es5001566.
Janssen, N., Hoek, G., Simic-Lawson, M., Fischer, P., Bree, L. van, Brink, H. ten, Keuken, M., Atkinson, R.W., Anderson, H.R., Brunekreef, B., Cassee, F.R., 2011. Black carbon as an additional indicator of the adverse health effects of airborne particles compared with PM10 and PM2.5. Environ. Health Perspect. 119, 12. https://doi.org/10.1289/ehp.1003369.
Järvinen, A., Aitomaa, M., Rostedt, A., Keskinen, J., Yli-Ojanperä, J., 2014. Calibration of the new electrical low pressure impactor (ELPI+). J. Aerosol Sci. 69, 150–159. https://doi.org/10.1016/j.jaero-sci.2013.12.006.
Jimenez, J.L., Jayne, J.T., Shi, Q., Kolb, C.E., Worsnop, D.R., Yourshaw, I., Seinfeld, J.H., Flagan, R.C., Zhang, X., Smith, K.A., Morris, J.W., Davidovits, P., 2003. Ambient Aerosol Sampling Using the Aerodyne Aerosol Mass Spectrometer, vol. 108. https://doi.org/10.1029/2001JD001213.
Jung, C.R., Lin, Y.T., Hwang, B.F., 2015. Ozone, particulate matter, and newly diagnosed Alzheimer's disease: a population-based cohort study in Taiwan. J Alzheimers Dis 44 (2), 573–584. https://doi.org/10.3233/JAD-140855.
Karttunen, S., Kurppa, M., Auvinen, M., Hellsten, A., Järvi, L., 2020. Large-eddy Simulation of the Optimal Street-Tree Layout for Pedestrian-Level Aerosol Particle Concentrations – A Case Study from a City-Boulevard, vol. X. Atmospheric Environment, p. 6. https://doi.org/10.1016/j.aeaoa.2020.100073.
Keskinen, J., Pietarinen, K., Lehtimäki, M., 1992. Electrical low pressure impactor. J. Aerosol Sci. 23 (4), 353–360. https://doi.org/10.1016/0021-8502(92)90004-F.
Keuken, M.P., Moerman, M., Zandveld, P., Henzing, J.S., Hoek, G., 2015. Total and size-resolved particle number and black carbon concentrations in urban areas near Schiphol airport (The Netherlands). Atmos. Environ. 104, 132–142. https://doi.org/10.1016/j.atmosenv.2015.01.015.
Kirchstetter, T., Novakov, T., Hobbs, P., 2004. Evidence that the spectral dependence of light absorption by aerosols is affected by organic carbon. J. Geophys. Res. Atmos. 109, 21. https://doi.org/10.1029/2004JD004999.
Kristensson, A., Rissler, J., Löndahl, J., Johansson, C., Swietlicki, E., 2013. Size-Resolved respiratory tract deposition of sub-micrometer aerosol particles in a residential area with wintertime wood combustion. Aerosol Air Qual. Res. 13, 24–35. https://doi.org/10.4209/aaqr.2012.07.0194.
Kumar, P., Robins, A., Vardoulakis, S., Britter, S., 2010. A review of the characteristics of nanoparticles in the urban atmosphere and the prospects for developing regulatory controls. Atmos. Environ. 44, 5035–5052. https://doi.org/10.1016/j.atmosenv.2010.08.016, 39.
Kuula, Kuuluvainen, J.H., Niemi, J.V., Saukko, E., Portin, H., Kousa, A., Aurela, M., Rönkkö, T., Timonen, H., 2020. Long-term sensor measurements of lung deposited surface area of particulate matter emitted from local vehicular and residential wood combustion sources. Aerosol. Sci. Technol. 54 (2), 190–202. https://doi.org/10.1080/02786826.2019.1668909.
Kuuluvainen, H., Rönkkö, T., Järvinen, A., Saari, S., Karjalainen, P., Lähde, T., Pirjola, L., Niemi, J.V., Hillamo, R., Keskinen, J., 2016. Lung deposited surface area size distributions of particulate matter in different urban areas. Atmos. Environ. 136, 105–113. https://doi.org/10.1016/j.atmosenv.2016.04.019.
Kuuluvainen, H., Karjalainen, P., Saukko, E., Ovaska, T., Sirviö, K., Honkanen, M., Olin, M., Niemi, S., Keskinen, J., Rönkkö, T., 2020. Nonvolatile ultrafine particles observed to form trimodal size distributions in non-road diesel engine exhaust. Aerosol. Sci. Technol. 54 (11), 1345–1358. https://doi.org/10.1080/02786826.2020.1783432.
Lelieveld, J., Evans, J., Fnais, M., et al., 2015. The contribution of outdoor air pollution sources to premature mortality on a global scale. Nature 525, 367–371. https://doi.org/10.1038/nature15371.
Lepistö, T., Kuuluvainen, H., Juuti, P., Järvinen, A., Arffman, A., Rönkkö, T., 2020. Measurement of the human respiratory tract deposited surface area of particles with an electrical low pressure impactor. Aerosol. Sci. Technol. https://doi.org/10.1080/02786826.2020.1745141.
Lepistö, T., Kuuluvainen, H., Lintusaari, H., Kuittinen, N., Salo, L., Helin, A., Niemi, J.V., Manninen, H.E., Timonen, H., Jalava, P., Saarikoski, S., Rönkkö, T., 2022. Connection between lung deposited surface area (LDSA) and black carbon (BC) concentrations in road traffic and harbour environments. Atmos. Environ. 272. https://doi.org/10.1016/j.atmosenv.2021.118931.
Li, X., Jin, L., Kan, H., 2019. Air pollution: a global problem needs local fixes Nature 570 (7762), 437–439. https://doi.org/10.1038/d41586-019-01960-7.
Lobo, P., Hagen, D.E., Whitefield, P.D., 2012. Measurement and analysis of aircraft engine PM emissions downwind of an active runway at the Oakland International Airport. Atmos. Environ. 61, 114–123. https://doi.org/10.1016/j.atmosenv.2012.07.028.

Luoma, K., Niemi, J.V., Aurela, M., Fung, P.L., Helin, A., Hussein, T., Kangas, L., Kousa, A., Rönkkö, T., Timonen, H., Virkkula, A., Petäjä, T., 2021. Spatiotemporal variation and trends in equivalent black carbon in the Helsinki metropolitan area in Finland. Atmos. Chem. Phys. 21, 1173–1189. https://doi.org/10.5194/acp-21-1173-2021.

Maher, B.A., Ahmed, Imad, Karloukovski, V., MacLaren, D.A., Foulds, P.G., Allsop, D., Mann, D.M.A., Torres-Jardón, R., Calderon-Garciduenas, L., 2016. Magnetite pollution nanoparticles in the human brain." edited by Y. Rudich. Proc. Natl. Acad. Sci. USA 113 (39), 10797–10801. https://www.pnas.org/content/113/39/10797.

Miller, M.R., Raftis, J.B., Langrish, J.P., McLean, S.G., Samutrtai, P., Connell, S.P., Wilson, S., Vesey, A.T., Fokkens, P.H.B., Boere, A. John F., Krystek, P., Campbell, C. J., Hadoke, P.W.F., Donaldson, K., Cassee, F.R., Newby, D.E., Duffin, R., Mills, N.L., 2017. ACS Nano 11 (5), 4542–4552. https://doi.org/10.1021/acsnano.6b08551.

Oberdorster, G., Oberdorster, E., Oberdorster, J., 2005. Nanotoxicology: an emerging discipline evolving from studies of ultrafine particles. Environ. Health Perspect. 113 (7), 823–839. https://doi.org/10.1289/ehp.7339.

Ohlwein, S., Kappeler, R., Kutlar Joss, M., et al., 2019. Health effects of ultrafine particles: a systematic literature review update of epidemiological evidence. Int. J. Publ. Health 64, 547–559. https://doi.org/10.1007/s00038-019-01202-7.

Onasch, T.B., Trimborn, A., Fortner, E.C., Jayne, J.T., Kok, G.L., Williams, L.R., Davidovits, P., Worsnop, D.R., 2012. Soot Particle Aerosol Mass Spectrometer, vol. 46. Development, Validation, pp. 804–817. https://doi.org/10.1080/02786826.2012.663948 and Initial Application.

Patel, S., Leavey, A., Sheshadri, A., et al., 2018. Associations between household air pollution and reduced lung function in women and children in rural southern India. J. Appl. Toxicol. 38, 1405–1415. https://doi.org/10.1002/jat.3659.

Pirjola, L., Niemi, J.V., Saarikoski, S., Aurela, M., Enroth, J., Carbone, S., Saarnio, K., Kuuluvainen, H., Kousa, A., Rönkkö, T., Hillamo, R., 2017. Physical and chemical characterization of urban winter-time aerosols by mobile measurements in Helsinki, Finland. Atmos. Environ. 158, 60–75. https://doi.org/10.1016/j.atmosenv.2017.03.028.

Rissler, J., Nordin, E.Z., Eriksson, A.C., Nilsson, P.T., Frosch, M., Sporre, M.K., Wierzbicka, A., Svenningsson, B., Löndahl, J., Messing, M.E., et al., 2014. Effective density and mixing state of aerosol particles in a near-traffic urban environment. Environ. Sci. Technol. 48 (11), 6300–6308. https://doi.org/10.1021/es5000353.

Rolph, G., Stein, A., Stunder, B., 2017. Real-time environmental applications and display sYstem: READY. Environ. Model. Software 95, 210–228. https://doi.org/10.1016/j.envsoft.2017.06.025.

Rönkkö, T., Pirjola, L., Ntziachristos, L., Heikkilä, J., Karjalainen, P., Hillamo, R., Keskinen, J., 2014. Environ. Sci. Technol. 48 (3), 2043–2050. https://doi.org/10.1021/es405687m.

Rönkkö, T., Kuuluvainen, H., Karjalainen, P., Keskinen, J., Hillamo, R., Niemi, J.V., Pirjola, L., Timonen, H.J., Saarikoski, S., Saukko, E., Järvinen, A., Silvennoinen, H., Rostedt, A., Olin, M., Yli-Ojanperä, J., Nousiainen, P., Kousa, A., Dal Maso, M., 2017. Traffic is a major source of atmospheric nanocluster aerosol. Proc. Natl. Acad. Sci. USA 114, 7549–7554. https://doi.org/10.1073/pnas.1700830114.

Saarikoski, S., Niemi, J.V., Aurela, M., Pirjola, L., Kousa, A., Rönkkö, T., Timonen, H., 2021. Sources of black carbon at residential and traffic environments obtained by two source apportionment methods. Atmos. Chem. Phys. 21, 14851–14869. https://doi.org/10.5194/acp-21-14851-2021.

Sandradewi, J., Prévôt, A.S.H., Szidat, S., Perron, N., Rami Alfarra, M., Lanz, V.A., Weingartner, E., Baltensperger, U., 2008. Using aerosol light absorption measurements for the quantitative determination of wood burning and traffic emission contributions to particulate matter. Environ. Sci. Technol. 42, 3316–3323. https://doi.org/10.1021/es702253m.

Schripp, T., Anderson, B., Crosbie, E.C., Moore, R.H., Herrmann, F., Oßwald, P., Wahl, C., Kapernaum, M., Köhler, M., Le Clercq, P., Rauch, B., Eichler, P., Mikoviny, T., Wisthaler, A., 2018. Environ. Sci. Technol. 52 (8), 4969–4978. https://doi.org/10.1021/acs.est.7b06244.

Segersson, D., Johansson, C., Forsberg, B., 2021. Near-source risk functions for particulate matter are critical when assessing the health benefits of local abatement strategies. Int. J. Environ. Res. Publ. Health 18 (13), 6847. https://doi.org/10.3390/ijerph18136847.

Sicard, P., Agathokleous, E., De Marco, A., et al., 2021. Urban population exposure to air pollution in Europe over the last decades. Environ. Sci. Eur. 33, 28. https://doi.org/10.1186/s12302-020-00450-2.

Stacey, B., 2019. Measurement of ultrafine particles at airports: a review. Atmos. Environ. 198, 463–477. https://doi.org/10.1016/j.atmosenv.2018.10.041.

Stein, A.F., Draxler, R.R., Rolph, G.D., Stunder, B.J.B., Cohen, M.D., Ngan, F., 2015. NOAA's HYSPLIT atmospheric transport and dispersion modeling system. Bull. Am. Meteorol. Soc. 96, 2059–2077. https://doi.org/10.1175/BAMS-D-14-00110.1.

Teinilä, K., Timonen, H., Aurela, M., Kuula, J., Rönkkö, T., Hellèn, H., Loukkola, K., Kousa, A., Niemi, J.V., Saarikoski, S., 2022. Characterization of particle sources and comparison of different particle metrics in an urban detached housing area. Finland, Atmospheric Environment 272, 118939. https://doi.org/10.1016/j.atmosenv.2022.118939.

Timonen, H., Mylläri, F., Simonen, P., Aurela, M., Maasikmets, M., Bloss, M., Kupri, H.-L., Vainumäe, K., Lepistö, T., Salo, L., et al., 2021. Household solid waste combustion with wood increases particulate trace metal and lung deposited surface area emissions. J. Environ. Manag. 293 https://doi.org/10.1016/j.jenvman.2021.112793.

Timonen, H., Carbone, S., Aurela, M., Saarnio, K., Saarikoski, S., Ng, N.L., Canagaratna, M.R., Kulmala, M., Kerminen, V.M., Worsnop, D.R., et al., 2013. Characteristics, sources and water-solubility of ambient submicron organic aerosol in springtime in Helsinki, Finland. J. Aerosol Sci. 56, 61–77. https://doi.org/10.1016/j.jaerosci.2012.06.005.

Todea, A.M., Beckmann, S., Kaminski, H., Asbach, C., 2015. Accuracy of electrical aerosol sensors measuring lung deposited surface are concentrations. J. Aerosol Sci. 89, 96–109. https://doi.org/10.1016/j.jaerosci.2015.07.003.

Torvela, T., Tissari, J., Sippula, O., Kaivosoja, T., Leskinen, J., Viren, A., Lähde, A., Jokiniemi, J., 2014. Effect of wood combustion conditions on the morphology of freshly emitted fine particles. Atmos. Environ. 87, 65e76.

Turgut, E.T., Gaga, E.O., Jovanović, G., et al., 2019. Elemental characterization of general aviation aircraft emissions using moss bags. Environ. Sci. Pollut. Res. 26, 26925–26938. https://doi.org/10.1007/s11356-019-05910-8.

Vohra, K., Vodonos, A., Schwartz, J., Marais, E.A., Sulprizio, M.P., Mickley, L.J., 2021. Global mortality from outdoor fine particle pollution generated by fossil fuel combustion: results from. GEOS-Chem, Environmental Research 195, 110754. https://doi.org/10.1016/j.envres.2021.110754. ISSN 0013-9351.

WHO (World Health Organization), 2021. WHO Global Air Quality Guidelines: Particulate Matter (PM2.5 and PM10), Ozone, Nitrogen Dioxide, Sulfur Dioxide and Carbon Monoxide. World Health Organization. https://apps.who.int/iris/handle/10665/345329. License: CC BY-NC-SA 3.0 IGO.

Willeke, K., Baron, P., 2005. Aerosol Measurement: Principles, Techniques, and Applications. Van Nostrand Reinhold, New York, USA.

Zotter, P., Herich, H., Gysel, M., El-Haddad, I., Zhang, Y., Močnik, G., Hüglin, C., Baltensperger, U., Szidat, S., Prévôt, A.S.H., 2017. Evaluation of the Absorption Ångström Exponents for Traffic and Wood Burning in the Aethalometer-Based Source Apportionment Using Radiocarbon Measurements of Ambient Aerosol, pp. 4229–4249. https://doi.org/10.5194/acp-17-4229-2017, 17.